

Thermodynamics of Optical Bloch Equations

Cyril Elouard,^{1,*} David Herrera-Martí,² Massimiliano Esposito,^{3,†} and Alexia Auffèves^{4,‡}

¹*Department of Physics and Astronomy, University of Rochester, Rochester, NY 14627, USA*

²*Atos Centre for Excellence in Performance Programming, 1 rue de Provence, 38130 Echirolles, France*

³*Complex Systems and Statistical Mechanics, Department of Physics and Materials Science, University of Luxembourg, L-1511 Luxembourg, Luxembourg*

⁴*CNRS and Université Grenoble Alpes, Institut Néel, F-38042 Grenoble, France*

(Dated: July 7, 2022)

Optical Bloch Equations (OBE) describe the coherent exchange of energy between a quantum emitter and a quasi-resonant field in the presence of a thermal reservoir. Despite it is an ubiquitous process in quantum technologies, a thermodynamical analysis is still missing. We hereby provide such an analysis. Our approach is based on a partial secular approximation applied on the dynamical equations of the full atom-bath system. We identify two regimes of parameters respectively leading to the OBE or the Floquet Master Equations (FME) and the consistent expressions the first and the second law of thermodynamics. In the regime where OBE are valid, we single out quantum signatures in the heat flows and in the entropy production, related to the creation of coherences by the driving field and their erasure by the bath. Our findings contribute to bridge an open gap between quantum thermodynamics and quantum optics.

I. INTRODUCTION

Optical Bloch Equations (OBE) are textbook equations in quantum optics that describe the dynamics of a quasi-resonantly driven quantum emitter coupled to a finite temperature bath. They have for long successfully modeled a broad range of experimental situations, both in the weak and strong regimes of driving. The latter regime captures the coherent and reversible exchange of energy between the quantum emitter and the drive - the celebrated Rabi oscillation [1]: As such, it is crucial for many functionalities of quantum technologies, e.g. the coherent manipulation of the quantum emitter's state, the implementation of quantum gates based on the resonant addressing of atomic transitions, or the amplification of light.

Despite their importance for quantum protocols, the OBE are still missing a consistent thermodynamical description. A key issue is that the dissipation term present in the OBE is similar to the one experienced by the bare atom, whichever the driving strength may be. OBE thus provide a typical example of “local master equations” where the dissipation terms are determined from only a subpart of the system's energy spectrum. The consistency of local master equations with the second law of thermodynamics has been much debated [2–5], and opposed to global master equations where the dissipation rates involve the full energy spectrum. These latter equations are by construction compliant with the so called Kubo-Martin-Schwinger (KMS) condition on the reservoir state [6], ensuring local detailed balance and thus thermodynamic consistency. In the context of resonance fluorescence, Floquet master equations (FME) [7–10] are

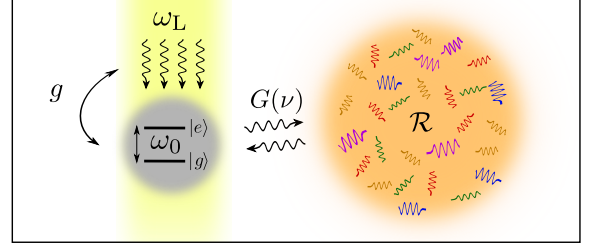


FIG. 1. A two-level atom of frequency ω_0 is driven by a quasi-resonant monochromatic field of frequency ω_L with a coupling strength g . The atom also interacts with a thermal bath \mathcal{R} at temperature T . The rate of photon exchange with the reservoir is set by the spectral density $G(\nu)$, i.e. the Fourier transform of the atom-bath correlation function (See text). **b** and **c**: Typical spectral widths at play. Orange solid line: $G(\nu)$, black solid line: energy spectrum of the resonantly driven atom composed of three peaks centered around ω_L and split by the Rabi frequency Ω (Mollow triplet).

such global master equations. However, FME are limited to coarse-graining times that largely overcome the Rabi period, blurring out the description of any coherent phenomenon. For this reason the coherent regime of light-matter interaction has remained largely unexplored in quantum thermodynamics.

In this article, we provide a consistent thermodynamical analysis of the OBE valid beyond the weak-driving regime, i.e where Rabi oscillations can be observed. To do so, we first propose a rigorous derivation of the OBE based on a partial secular approximation, that is fully consistent with the KMS condition. In the regime where both the FME and the OBE are valid descriptions, we prove that the FME can be derived from a coarse-graining in time of the OBE. Then, starting from a full system-bath formulation of thermodynamics [11] and consistently implementing the approximation scheme

* cyril.elouard@gmail.com

† massimiliano.esposito@uni.lu

‡ alexia.auffeves@neel.cnrs.fr

used when deriving the OBE, we compute the heat flow in terms of the OBE and the other thermodynamic quantities entering the first and second laws of thermodynamics. Finally, we single out and fully characterize a genuinely quantum out-of-equilibrium situation captured by the OBE, where coherences built by the drive in the free atom energy eigenbasis are continuously removed by the thermal bath. This new regime can be revealed by observable quantum thermodynamical signatures in the heat flow and entropy production. Our results contribute to bridge an important gap between quantum thermodynamics and quantum optics and the methods we use can be generalised to driven open quantum system with more than two-levels.

II. DRIVEN ATOM MASTER EQUATION

A. Microscopic derivation

1. Model

We consider a driven two-level atom described by the Hamiltonian $H(t) = H_0 + V(t)$, where $H_0 = \hbar\omega_0\sigma_z/2$ is the free Hamiltonian of the atom. Instead, $V(t) = \frac{\hbar g}{2} \cos(\omega_L t) (\sigma_- + \sigma_+)$ captures the effect of the driving by a quasi-resonant classical source of frequency $\omega_L = \omega_0 - \delta$ where $|\delta| \ll \omega_0$ is the detuning (See Fig.1). We introduced the Pauli matrix $\sigma_z = |e\rangle\langle e| - |g\rangle\langle g|$ and the lowering operator $\sigma_- = |g\rangle\langle e| = \sigma_+^\dagger$, where $|e\rangle$ and $|g\rangle$ are the excited and ground states of the atom, respectively. The light matter coupling strength verifies $g \ll \omega_0, \omega_L$, justifying to work within the Rotating Wave Approximation [1] and to use $V(t) \simeq \hbar g (e^{i\omega_L t} \sigma_- + e^{-i\omega_L t} \sigma_+)$, with $\omega_L > 0$.

The atom is coupled to an electromagnetic reservoir \mathcal{R} modeled by a collection of harmonic oscillators, described by the Hamiltonian $H_{\mathcal{R}} = \sum_k \hbar\omega_k (a_k^\dagger a_k + 1/2)$, where a_k is the lowering operator in the bosonic mode k of the reservoir that has frequency ω_k . The reservoir is assumed to be in thermal equilibrium at temperature T as described by the state $\rho_{\mathcal{R}}^{\text{eq}} = e^{-H_{\mathcal{R}}/T}/Z_{\mathcal{R}}$. The atom-reservoir coupling is described by the Hamiltonian $H_{S\mathcal{R}} = R\sigma_x$, where $R = \sum_k \hbar g_k (a_k^\dagger + a_k)$ is a reservoir operator. The coupling strengths g_k are taken real without loss of generality. The density operator $\rho_{S\mathcal{R}}$ of the global system obeys the exact Liouville-Von Neumann equation:

$$\dot{\rho}_{S\mathcal{R}}(t) = -\frac{i}{\hbar} [H(t) + H_{S\mathcal{R}}(t) + H_{\mathcal{R}}, \rho_{S\mathcal{R}}(t)]. \quad (1)$$

Both OBE and FME rely on the assumption that the coupling between the reservoir and the system is weak enough such that the total density operator $\rho_{S\mathcal{R}}$ evolves slowly when written in the appropriate interaction picture. This new frame is reached via two successive transformations. First, one goes to the rotating frame by ap-

plying the unitary transformation $U_{\text{rot}} = e^{it\omega_L\sigma_z/2}$. An operator in the rotating frame is denoted by a tilde, e.g. the total density operator in rotating frame is $\tilde{\rho}_{S\mathcal{R}}(t) = U_{\text{rot}}\rho_{S\mathcal{R}}(t)U_{\text{rot}}^\dagger$ and using Eq. (1) its evolution reads

$$\dot{\tilde{\rho}}_{S\mathcal{R}}(t) = -\frac{i}{\hbar} [\tilde{H}_{\text{eff}} + \tilde{H}_{S\mathcal{R}}(t) + H_{\mathcal{R}}, \tilde{\rho}_{S\mathcal{R}}(t)], \quad (2)$$

where $\tilde{H}_{\text{eff}} = U_{\text{rot}}H(t)U_{\text{rot}}^\dagger - \frac{\hbar\omega_L}{2}\sigma_z = \frac{\hbar\delta}{2}\sigma_z + \frac{\hbar g}{2}\sigma_x$ is the effective Hamiltonian of the atom in the rotating frame (the term $-\frac{\hbar\omega_L}{2}\sigma_z$ comes from the time-dependence of the transformation U_{rot}) and $\tilde{H}_{S\mathcal{R}}(t) = R(\sigma_- e^{-i\omega_L t} + \sigma_+ e^{i\omega_L t})$. Second, one goes to the interaction picture with respect to $\tilde{H}_{\text{eff}} + H_{\mathcal{R}}$, using the unitary transformation $U_{\text{int}} = e^{it(\tilde{H}_{\text{eff}} + H_{\mathcal{R}})}$. Using the superscript I to denote the result of the two successive transformations, we get e.g. $\rho_{S\mathcal{R}}^I(t) = U_{\text{int}}\tilde{\rho}_{S\mathcal{R}}(t)U_{\text{int}}^\dagger$ with the corresponding evolution equation

$$\dot{\rho}_{S\mathcal{R}}^I(t) = -\frac{i}{\hbar} [\tilde{H}_{S\mathcal{R}}^I(t), \rho_{S\mathcal{R}}^I(t)], \quad (3)$$

where $\tilde{H}_{S\mathcal{R}}^I(t) = U_{\text{int}}\tilde{H}_{S\mathcal{R}}(t)U_{\text{int}}^\dagger$.

It is useful for the following to introduce the spectral decomposition of \tilde{H}_{eff} . Its two eigenstates (which are often referred to as the state of the atom dressed by the driving field) are given by:

$$|+\rangle = \frac{\sqrt{\Omega + \delta}}{\sqrt{2\Omega}}|e\rangle + \frac{\sqrt{\Omega - \delta}}{\sqrt{2\Omega}}|g\rangle \quad (4a)$$

$$|-\rangle = -\frac{\sqrt{\Omega - \delta}}{\sqrt{2\Omega}}|e\rangle + \frac{\sqrt{\Omega + \delta}}{\sqrt{2\Omega}}|g\rangle, \quad (4b)$$

and are associated with the eigenvalues $\pm\Omega/2$, where

$$\Omega = \sqrt{g^2 + \delta^2} \quad (5)$$

is the Rabi frequency.

2. Properties of the bath

As in the standard case of a non-driven weakly dissipative quantum system [6], typical rate of evolution of the atom density operator due to the reservoir is determined by the spectral density $G(\nu)$ of the reservoir, defined as the Fourier transform of the atom-reservoir correlation function:

$$G(\nu) = \frac{1}{\hbar^2} \int_{-\infty}^{\infty} d\tau e^{i\nu\tau} \langle R^I(\tau)R^I(0) \rangle. \quad (6)$$

We have introduced the correlation function $\langle R^I(\tau)R^I(0) \rangle = \text{Tr}\{R^I(\tau)R^I(0)\rho_{\mathcal{R}}^{\text{eq}}\}$. Using the specific form of operator R and of the reservoir's equilibrium state $\rho_{\mathcal{R}}^{\text{eq}}$, we can derive the explicit form of $G(\nu)$. Noting that $\text{Tr}\{\rho_{\mathcal{R}}^{\text{eq}}a_j^\dagger a_k\} = \delta_{j,k}N(\omega_k)$, where we have introduced the Bose-Einstein distribution

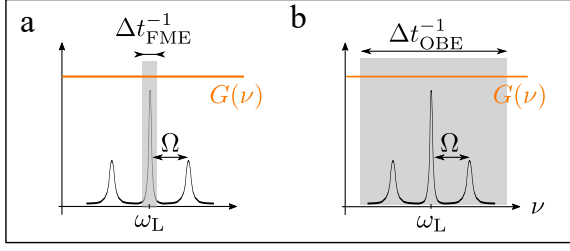


FIG. 2. **a**: FME regime. The coarse graining time verifies $\Delta t_{\text{FME}} \gg \Omega^{-1}$: The components of the Mollow triplet are resolved, but no Rabi oscillations can be observed. **b**: OBE regime. The coarse graining time verifies $\Delta t_{\text{OBE}} \ll \Omega^{-1}$: The components of the Mollow triplet are not resolved, but the Rabi oscillations can be observed.

$N(\nu) = [e^{\hbar\nu/k_B T} - 1]^{-1}$, and that $\text{Tr}\{\rho_{\mathcal{R}}^{\text{eq}} a_j a_k\} = 0$, we get:

$$\frac{G(\nu)}{2} = \Theta(\nu)\Gamma(\nu)(N(\nu) + 1) + \Theta(-\nu)\Gamma(-\nu)N(-\nu) \quad (7)$$

with $\Theta(\nu)$ the Heaviside function. We also defined

$$\Gamma(\nu) = \sum_k g_k^2 \delta_D(\nu - \omega_k), \quad (8)$$

with $\delta_D(\nu)$ denoting the Dirac distribution. It is straightforward to check that $G(-\nu) = e^{-\hbar\nu/k_B T} G(\nu)$, i.e. that $G(\nu)$ complies with the Kubo-Martin-Schwinger (KMS) condition [12, 13], as expected for a reservoir at thermal equilibrium. This plays an important role in ensuring that the obtained master equation is thermodynamically consistent [6]. Finally, the reservoir is characterized by a correlation time τ_c , defined as the typical decay time of the correlation function $\langle R^I(t) R^I(0) \rangle$.

3. Coarse-graining procedure

Our derivation of the driven-atom master equation is based on a coarse-graining in time of the exact evolution equation of the driven atom and the environment [1]. The typical rate of decay of the atom induced by the environment (in other words the time-scale of variation of $\rho_{\mathcal{SR}}^I$) is given by

$$G(\omega_0) = \gamma(\bar{n} + 1), \quad (9)$$

where

$$\gamma = \Gamma(\omega_0) \quad \text{and} \quad \bar{n} = N(\omega_0) \quad (10)$$

are the spontaneous emission rate of the bare (undriven) atom and the thermal occupation of the reservoir at the transition frequency of the bare atom, respectively [1]. If the time-scale $G^{-1}(\omega_0)$ is much larger than the correlation time of the reservoir τ_c , it is possible to obtain a Markovian master equation for the atom alone from

a coarse-graining in time of Eq. (3) over a time-scale $\tau_c \ll \Delta t_{\text{cg}} \ll G(\omega_0)^{-1}$, followed by a trace over the reservoir. Only terms up to second order in the coupling Hamiltonian, which have typical magnitude $G(\omega_0)\Delta t$, are kept. The procedure, presented generically in Ref. [1], yields an equation similar to Redfield equation [14] for the density operator $\rho(t) = \text{Tr}_{\mathcal{R}}\{\rho_{\mathcal{SR}}(t)\}$ of the atom:

$$\dot{\rho}^I(t) = -\frac{1}{\hbar^2 \Delta t_{\text{cg}}} \int_t^{t+\Delta t_{\text{cg}}} dt' \int_t^{t'} dt'' \text{Tr}_{\mathcal{R}} \left\{ [H_{\mathcal{SR}}^I(t'), [H_{\mathcal{SR}}^I(t''), \rho_{\mathcal{SR}}^I(t'')]] \right\}. \quad (11)$$

Note that it was also assumed without loss of generality that the expectation value of $H_{\mathcal{SR}}$ in the reservoir equilibrium state is zero [1, 15], such that there remains no first order contribution in the coupling Hamiltonian. We further simplify Eq. (11) by applying the Born-Markov approximation [1, 6]: We replace $\rho_{\mathcal{SR}}^I(t'')$ by $\rho^I(t) \otimes \rho_{\mathcal{R}}^{\text{eq}}$ inside the double integration, assuming the reservoir to be in the equilibrium state $\rho_{\mathcal{R}}^{\text{eq}}$. The exact expression of $H_{\mathcal{SR}}^I(t)$ is obtained by identifying the Fourier components of $\sigma_l^I(t) = e^{i\omega_L t} \sum_{\omega} \sigma_l(\omega) e^{i\omega t}$, for $l = \pm$, in terms of the eigenstates of \tilde{H}_{eff} , defined in Eqs. (4a)-(4b). We obtain:

$$\sigma_{\pm}(0) = \frac{g}{2\Omega} (|+\rangle\langle+| - |-\rangle\langle-|) \quad (12a)$$

$$\sigma_{\pm}(-\Omega) = \mp \frac{\Omega \mp \delta}{2\Omega} |-\rangle\langle+| \quad (12b)$$

$$\sigma_{\pm}(\Omega) = \pm \frac{\Omega \pm \delta}{2\Omega} |+\rangle\langle-|, \quad (12c)$$

such that $H_{\mathcal{SR}}^I(t) = R^I(t) \sum_{l=\pm} \sum_{\omega=0, \pm\Omega} \sigma_l(\omega) e^{i\omega_L t} e^{i\omega t}$. Finally, Eq. (11) can be rewritten with the explicit expression of $H_{\mathcal{SR}}^I(t)$, leading to:

$$\begin{aligned} \dot{\rho}^I(t) = & \frac{1}{4\Delta t_{\text{cg}}} \int_t^{t+\Delta t_{\text{cg}}} dt' \sum_{l'l'} \sum_{\omega, \omega'} e^{i(\omega-\omega')t' + i(l-l')\omega_L t'} \\ & \times G(-\omega - l\omega_L) \left[\sigma_l(\omega) \rho^I(t) \sigma_{l'}^\dagger(\omega') - \sigma_{l'}^\dagger(\omega') \sigma_l(\omega) \rho^I(t) \right] + \text{h.c.} \end{aligned} \quad (13)$$

To go to Eq. (13), the integral over t'' in Eq. (11) was turned into an integral over $\tau = t' - t''$, whose upper limit can be approximated by $+\infty$ as the argument of the integration contains the correlation function $\langle R^I(0) R^I(\tau) \rangle$ which decays for $\tau \gg \tau_c$ [1, 6]. We have also ignored the imaginary part of $\int_0^\infty d\tau e^{i\nu\tau} \langle R^I(\tau) R^I(0) \rangle$ which contributes to the Lamb and dynamic Stark shifts, small corrections to the free atom frequency [16, 17] (see Appendix A).

Eq.(13) is not ensured to be completely positive since it is not yet in the Lindblad form [18]. The derivation therefore requires an additional step, called Secular Approximation [1], which allows us to get rid of terms rapidly oscillating with time t' over frequencies much larger than $\Delta t_{\text{cg}}^{-1}$ as they will average out in the integration over t' . In order to get a positive master equation, one therefore needs to choose Δt_{cg} large enough such that the only remaining terms form a Lindblad equation.

B. The global approach: the FME

1. Derivation and dynamics

A sufficient – but in general, not necessary – solution to obtain a Lindblad equation consists in choosing Δt_{cg} much larger than any oscillation frequency involved in the interaction-picture system operators $\sigma_l^I(t)$. This method was introduced in Ref. [19] for systems characterized by a time-independent Hamiltonian. In the context of multipartite systems, it leads to so-called “global” master equations characterized by a dissipation term which depends on the energy spectrum of the total system [4]. In the present case, it consists in choosing $\Delta t_{\text{cg}} \equiv \Delta t_{\text{FME}}$ (See Fig.2) verifying

$$\tau_c^{-1}, \omega_L, \omega_0, \Omega \gg \Delta t_{\text{FME}}^{-1} \gg G(\omega_0), \quad (14)$$

in order to suppress all the terms with $l \neq l'$ and $\omega \neq \omega'$ in Eq.(13). This procedure yields a master equation in the Lindblad form that is known as Floquet Master Equation (FME). In this Section we briefly review this approach in order to stress its connections with the OBE description.

The long coarse-graining is sufficient to resolve all the frequencies of the emission and absorption spectra of the atom, i.e. $\omega + l\omega_L$, with $\omega = 0, \pm\Omega$ and $l = \pm$ (see Fig. 2), leading to a Lindbladian that depends on all these frequencies. The equation obtained once the explicit expressions of the operators $\sigma_l(\omega)$ and spectral density $G(\nu)$ are introduced is more simply written in the frame rotating at the drive frequency, and in the dressed basis $|\pm\rangle$ of the atom. It takes the form $\dot{\rho}(t) = -i[\tilde{H}_{\text{eff}}, \rho(t)] + \tilde{\mathcal{L}}_{\text{FME}}[\rho(t)]$, where $\tilde{\mathcal{L}}_{\text{FME}} = \tilde{\mathcal{L}}_0 + \tilde{\mathcal{L}}_1 + \tilde{\mathcal{L}}_2$, is composed of the three superoperators

$$\tilde{\mathcal{L}}_0 = (\gamma_{0,\downarrow} + \gamma_{0,\uparrow})\mathcal{D}_{\Sigma_z} \quad (15)$$

$$\tilde{\mathcal{L}}_1 = \gamma_{1,\downarrow}\mathcal{D}_{\Sigma_-} + \gamma_{1,\uparrow}\mathcal{D}_{\Sigma_+} \quad (16)$$

$$\tilde{\mathcal{L}}_2 = \gamma_{2,\downarrow}\mathcal{D}_{\Sigma_-} + \gamma_{2,\uparrow}\mathcal{D}_{\Sigma_+}, \quad (17)$$

which involve the Pauli matrices $\Sigma_z = |+\rangle\langle+| - |-\rangle\langle-|$ and $\Sigma_- = |-\rangle\langle+| = \Sigma_+^\dagger$ in the dressed basis. We also denoted $\mathcal{D}_X[\rho] = X\rho X^\dagger - \frac{1}{2}\{X^\dagger X, \rho\}$, with $\{A, B\} = AB + BA$, the dissipation superoperator.

The Lindbladian $\tilde{\mathcal{L}}_{\text{FME}}$ reflects the interplay between the driving and the dissipation on time-scales larger than Δt_{FME} . The three different terms it contains can be interpreted the following way: $\tilde{\mathcal{L}}_0$ corresponds to the Lindbladian of a pure-dephasing channel (in the dressed basis), involving the rates:

$$\gamma_{0,\downarrow} = \frac{g^2}{4\Omega^2}\Gamma(\omega_L)(N(\omega_L) + 1) \quad (18)$$

$$\gamma_{0,\uparrow} = \frac{g^2}{4\Omega^2}\Gamma(\omega_L)N(\omega_L). \quad (19)$$

$\tilde{\mathcal{L}}_1$ and $\tilde{\mathcal{L}}_2$ correspond to two thermal relaxation channels

in the dressed basis involving the rates

$$\gamma_{1,\downarrow} = \frac{(\Omega + \delta)^2}{4\Omega^2}\Gamma(\omega_1)(N(\omega_1) + 1) \quad (20)$$

$$\gamma_{1,\uparrow} = \frac{(\Omega + \delta)^2}{4\Omega^2}\Gamma(\omega_1)N(\omega_1) \quad (21)$$

$$\gamma_{2,\downarrow} = \frac{(\Omega - \delta)^2}{4\Omega^2}\Gamma(\omega_2)N(\omega_2) \quad (22)$$

$$\gamma_{2,\uparrow} = \frac{(\Omega - \delta)^2}{4\Omega^2}\Gamma(\omega_2)(N(\omega_2) + 1), \quad (23)$$

where we have introduced the frequencies $\omega_1 = \omega_L + \Omega$ and $\omega_2 = \omega_L - \Omega$. Together with ω_L (associated with decay channel $\tilde{\mathcal{L}}_0$), they constitute the three effective transitions frequencies seen by the reservoir in the atom dressed by the driving field. They also match the three frequencies of the fluorescence emission spectrum, the famous Mollow triplet [20].

An intuitive explanation for the origin of these three frequencies can be obtained from the radiative cascade picture [1]. This description is obtained when the driving field is modeled quantum mechanically as an effective single-mode cavity of frequency ω_L initialized in a large amplitude coherent field. The FME are recovered from this picture by tracing over the field degree of freedom. The cavity-atom energy diagram is a quasi periodic ladder involving two-state manifolds $\{|+(n_L)\rangle, |-(n_L)\rangle\}$, labeled by the number of photons in the cavity n_L . The reservoir induces transitions between the levels of manifolds n_L and $n_L \pm 1$ which are separated by energy splittings $\hbar\omega_{1,2}$ and $\hbar\omega_L$. When focusing on the dynamics of the atom alone as the FME do, one sees instead transitions induced by the reservoir between the dressed states. These transitions are assisted by the driving field which provides or takes a photon of frequency ω_L each time a photon is emitted or absorbed. The frequencies $\omega_{1,2}$ and ω_L are then formed as the the sum of the transition frequency in the driving field $\pm\omega_L$ and that in the atom $\omega \in \{0, \pm\Omega\}$ (see Fig. 3). This picture also explains the apparent negative temperature of channel \mathcal{L}_2 (resulting in $\gamma_{2,\downarrow} \leq \gamma_{2,\uparrow}$) as an artifact of the reduction of the periodic ladder onto the two-level atom subspace. We finally emphasize that while we started our study with a classical description of the driving field (only via driving Hamiltonian $V(t)$), the role of the field in assisting the transition between dressed states is still captured and can be tracked back to be a consequence of the time-oscillating coefficients in $V(t)$.

2. Dynamics in the dressed basis and steady state

The choice of a long coarse-graining time Δt_{FME} yields an equation in which the dissipation solely involves transitions between the eigenstates of the atom dressed by the driving field, i.e. the eigenstates of \tilde{H}_{eff} . This implies that when the FME is expressed in the dressed basis, the dynamic of the populations is not coupled to

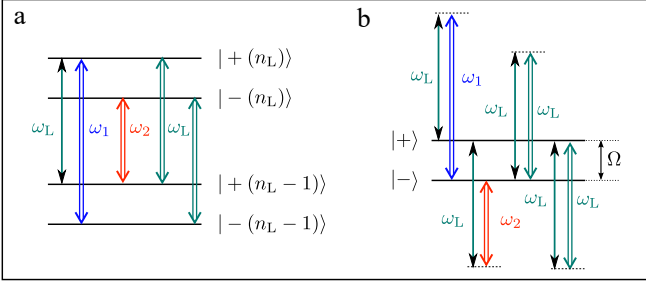


FIG. 3. Interpretation of Floquet dynamics. a) Energy diagram of the joint system field-atom when the field is modeled by a cavity mode (radiative cascade picture). The frequencies $\omega_{1,2}$ and ω_L appear as the allowed transitions between these joint eigenstates. b) The FME involve transitions between the dressed states that are assisted by the driving field which can provide or take a single quantum of energy $\hbar\omega_L$. They can be deduced from the radiative cascade model by tracing over the field subspace.

the coherences, and corresponds to a rate equation that could model a classical stochastic process. The coherences evolve according to another set of dynamical equations whose solution exhibit exponential decay to zero.

The steady state $\tilde{\rho}_{\text{FME}}^\infty = \tilde{P}_+^\infty |+\rangle\langle+| + (1 - \tilde{P}_+^\infty) |-\rangle\langle-|$ of the total master equation is therefore diagonal in the dressed basis and verifies:

$$\tilde{P}_+^\infty = \langle+|\tilde{\rho}_{\text{FME}}^\infty|+\rangle = \frac{\gamma_{1,\uparrow} + \gamma_{2,\uparrow}}{\gamma_{1,\uparrow} + \gamma_{1,\downarrow} + \gamma_{2,\uparrow} + \gamma_{2,\downarrow}}. \quad (24)$$

It is also the fixed point of the Lindbladian \mathcal{L}_{FME} alone. This property – together with the fact that all the transition rates are related two by two with a detailed balance condition involving the frequencies $\omega_{1,2}$ and ω_L – leads to a transparent thermodynamic interpretation of the FME (see Section III C). It is therefore natural that the FME was first used to study the thermodynamics of fluorescence [7–10]. However, this approach is limited since it solely captures the dynamics of the system on timescales much longer than a single Rabi period Ω^{-1} , blurring out the description of Rabi oscillations and causing the emergence of the classical-like rate equation for the population only. Consequently, the coherent regime of light-matter interaction has remained unexplored by quantum thermodynamics so far.

C. The OBE

1. Regime of validity

The OBE have been historically justified by the assumption that the presence of the drive does not affect

the form of the dissipation [1]. While this assumption is natural for very a weak drive $g \ll \gamma$, demonstrating its validity in the regime of strong driving requires more care and its validity was debated until recently [21, 22]. In order to circumvent the limitations associated with the FME without performing such a seemingly crude approximation, we start from the precursor Eq. (13) and choose a shorter coarse-graining time Δt_{OBE} that fulfills:

$$\tau_c^{-1}, \omega_L, \omega_0 \gg \Delta t_{\text{OBE}}^{-1} \gg \Omega, \gamma. \quad (25)$$

It imposes $\omega_L \gg \Omega$ – which rules out the ultra-strong coupling regime between the driving field and the atom – while still encompassing a large range of parameter from weak to strong drive (i.e. Ω can be smaller or larger than γ).

The condition $\tau_c^{-1} \gg \Omega$ in Ineq. (25) can be recast in terms of the spectral density $G(\nu)$ being approximately flat on the two intervals $[\pm\omega_0 - \Omega, \pm\omega_0 + \Omega]$. We emphasize that this condition is different from the so-called singular coupling limit [15, 23], that involves a δ -correlated correlation function of operator $R^I(t)$, and therefore a completely flat spectral density. The latter approximation can be used to justify the form of the OBE, but was pointed out as being in contradiction with the KMS condition, which is essential for the thermodynamic validity of the OBE [21].

Conversely, the derivation presented here assumes the spectral density to be flat on each of the two intervals, but allows it to take two different values for positive and negative transition frequencies, respectively $G(\omega_0)$ and $G(-\omega_0)$. These two values verify $G(\omega_0) = e^{\hbar\omega_0/k_B T} G(-\omega_0)$. This behavior is consistent with the KMS condition even when associated with the condition with $\tau_c^{-1} \gg \Omega$. As the frequency τ_c^{-1} typically corresponds to the minimum of the environment bandwidth and $k_B T/\hbar$ [6], Ineq. (25) also implies that $\hbar\Omega \ll k_B T$, such that for $|\nu - \omega_0| \lesssim \Omega$, we have $G(\nu) = e^{\hbar\nu/k_B T} G(-\nu) + \mathcal{O}(\hbar\Omega/k_B T)$.

This analysis reveals that the treatment of a strictly zero temperature reservoir is actually forbidden. Rigorously, the regime of quantum optics thus corresponds to $\hbar\omega_0 \gg k_B T \gg \hbar\Omega$ where thermal occupation of the reservoir at the atomic frequency can be neglected, but the correlation time of the reservoir can still be considered as shorter than a Rabi period. The OBE have been rigorously derived in this limit ([17] section 2.3.2). We provide below a general derivation conserving the dependence on the thermal occupations.

2. Derivation

Using $\omega_L \Delta t_{\text{OBE}} \gg 1$, we can neglect in Eq.(13) the terms with $l \neq l'$ but keep the terms $\omega \neq \omega'$ (partial secular approximation), obtaining:

$$\begin{aligned} \dot{\rho}^I(t) = & \frac{1}{2\Delta t_{\text{cg}}} \int_t^{t+\Delta t_{\text{cg}}} dt' \sum_{\omega} e^{i\omega t'} \Gamma(\omega_L - \omega) N(\omega_L - \omega) \left(\sigma_+(\omega) \rho^I(t) \sigma_-^I(t') - \sigma_-^I(t') \sigma_+(\omega) \rho^I(t) \right) \\ & + \frac{1}{2\Delta t_{\text{cg}}} \int_t^{t+\Delta t_{\text{cg}}} dt' \sum_{\omega} e^{i\omega t'} \Gamma(\omega_L - \omega) (N(\omega_L - \omega) + 1) \left(\sigma_-(\omega) \rho^I(t) \sigma_+^I(t') - \sigma_+^I(t') \sigma_-(\omega) \rho^I(t) \right) + \text{h.c.} \end{aligned} \quad (26)$$

We have made use of the identity $\sum_{\omega'} \sigma_l(\omega') e^{i\omega' t'} e^{i\omega_L t'} = \sigma_l^I(t')$. If one stops the derivation at this point and write Eq. (26) in the Schrödinger picture, one obtains the Generalized Bloch Equations (GBE) as introduced in [22]. These equations can be written in a Lindblad form, and allow to describe the evolution of the atom over short time-scale, while still taking into account the local variations of reservoir spectral density, e.g. due to the differences of thermal occupations $N(\omega_L - \omega)$ for the three different values of ω . The resulting equation is still global as it involves the spectral density of the reservoir evaluated at all the transition frequencies of Hamiltonian \tilde{H}_{eff} . However, in the conditions captured by Ineq. (25) and in the absence of resonances in the reservoir spectrum nearby ω_0 , Eq. (26) can be further simplified. Indeed, $N(\omega_L - \omega)$ can be safely replaced with $N(\omega_0)$ as soon as either $\hbar\omega_0 \gg k_B T$ or $\hbar\Omega \ll k_B T$. Because of the inequality $\omega_0 \gg \Omega$, at least one of these inequalities is always satisfied, such that it is legitimate to do this replacement. On the other hand, the absence of resonances implies that $\Gamma(\omega_L - \omega) \simeq \Gamma(\omega_0)$ for all $\omega \in \{0, \pm\Omega\}$. When applying these approximations to Eq. (26), and then computing the sum over ω , we get:

$$\begin{aligned} \dot{\rho}^I(t) = & \frac{\gamma\bar{n}}{\Delta t_{\text{OBE}}} \int_t^{t+\Delta t_{\text{OBE}}} dt' \mathcal{D}_{\sigma_+^I(t')} [\rho^I(t)] \\ & + \frac{\gamma(\bar{n}+1)}{\Delta t_{\text{OBE}}} \int_t^{t+\Delta t_{\text{OBE}}} dt' \mathcal{D}_{\sigma_-^I(t')} [\rho^I(t)]. \end{aligned} \quad (27)$$

When rewritten in Schrödinger picture and once the (harmless) integration over t' is performed, Eq. (27) finally takes the well-known form of the OBE, namely:

$$\dot{\rho}(t) = -\frac{i}{\hbar} [H(t), \rho(t)] + \mathcal{L}_{\text{OBE}}[\rho(t)], \quad (28)$$

where \mathcal{L}_{OBE} the Lindbladian superoperator encoding the non-unitary part of the dynamics:

$$\mathcal{L}_{\text{OBE}}[\rho] = \gamma\bar{n}\mathcal{D}_{\sigma_+}[\rho] + \gamma(\bar{n}+1)\mathcal{D}_{\sigma_-}[\rho]. \quad (29)$$

D. Properties of the dynamics

In the rotating frame, the OBE take the form:

$$\dot{\tilde{\rho}}(t) = -\frac{i}{\hbar} [\tilde{H}_{\text{eff}}, \tilde{\rho}(t)] + \mathcal{L}_{\text{OBE}}[\tilde{\rho}(t)], \quad (30)$$

From Eqs. (30), one can note a crucial difference with the FME, which is that the dissipative part $\mathcal{L}_{\text{OBE}}[\tilde{\rho}(t)]$ and the unitary part $-\frac{i}{\hbar} [\tilde{H}_{\text{eff}}, \tilde{\rho}(t)]$ of the master equation have incompatible eigenbases. More precisely, in the bare atomic basis $\{|e\rangle, |g\rangle\}$, the dissipation exhibits the structure of rate equation which does not couple populations and coherences. But in this basis, the Hamiltonian \tilde{H}_{eff} is not diagonal and induces coherences. This implies that in contrast with the FME, the OBE cannot take the form of a rate equation in any basis, neither the eigenbasis of $H(t)$, that of \tilde{H}_{eff} or the bare atomic basis, and cannot be interpreted as a classical stochastic process.

E. FME versus OBE

In this section, we show that in the regimes in which both the FME and the OBE are valid, the FME can be deduced from the OBE via a coarse-graining procedure. We start from the OBE in the interaction picture with respect to \tilde{H}_{eff} , i.e.:

$$\dot{\rho}^I(t) = \gamma(\bar{n}+1)\mathcal{D}_{\sigma_-^I(t)}[\rho^I(t)] + \gamma\bar{n}\mathcal{D}_{\sigma_+^I(t)}[\rho^I(t)]. \quad (31)$$

We now coarse-grain this master equation choosing the time-scale leading to the FME, i.e. Δt_{FME} fulfilling Ineq. (14). We obtain:

$$\begin{aligned} \rho^I(t + \Delta t_{\text{FME}}) - \rho^I(t) = & \int_t^{t+\Delta t_{\text{FME}}} dt' \left(\gamma(\bar{n}+1)\mathcal{D}_{\sigma_-^I(t')} + \gamma\bar{n}\mathcal{D}_{\sigma_+^I(t')} \right) \rho^I(t'). \end{aligned} \quad (32)$$

As in the first coarse-graining procedure of Section II A, the evolution of the atom density matrix in the interaction picture $\rho^I(t)$ can be neglected over time-scale Δt_{FME} and we therefore replace $\rho^I(t')$ with $\rho^I(t)$ in the integrand of Eq.(32). We then use the Fourier decomposition of $\sigma_{\pm}^I(t)$ (see Eqs. (12a)-(12c)), and expand the terms $\mathcal{D}_{\sigma_{\pm}^I(t')}$ of the integrand of Eq.(32). Written in the dressed basis, we collect the terms proportional to $\mathcal{D}_{\Sigma_{\pm}^I(t')}$ and $\mathcal{D}_{\Sigma_z^I(t')}$, and other “non-diagonal” terms featuring oscillating coefficients $e^{\pm i\Omega t'}$ or $e^{\pm 2i\Omega t'}$. Such fast oscillations average to zero over $\Delta t_{\text{FME}} \gg \Omega^{-1}$. Neglecting these terms (which is equivalent to the secular ap-

	Optical Bloch Equations / Generalized Bloch Equations	Floquet Master Equation
Regime of validity	$\tau_c^{-1}, \omega_L, \omega_0^{-1} \gg \Omega, \gamma$	$\tau_c^{-1}, \omega_L, \omega_0, \Omega \gg \gamma$
Coarse-graining time Δt_{cg}	$\tau_c^{-1}, \omega_L, \omega_0 \gg \Delta t_{OBE}^{-1} \gg \Omega, \gamma$	$\tau_c^{-1}, \omega_L, \omega_0, \Omega \gg \Delta t_{FME}^{-1} \gg \gamma$
Other assumptions	$T \gg \hbar\Omega/k_B$, $G(\nu)$ flat on $[\omega_L - \Omega, \omega_L + \Omega]$ for $l = \pm$	$\Omega \ll \gamma\bar{n}$

TABLE I. Regime of validity of OBE/GBEs and FME.

proximation needed to derive the FME), we finally find:

$$\begin{aligned} \dot{\rho}^I(t) = & \gamma \left[\frac{\Omega^2 + \delta^2}{4\Omega^2} \bar{n} + \frac{(\Omega + \delta)^2}{4\Omega^2} \right] \mathcal{D}_{\Sigma_-} \\ & + \gamma \left[\frac{\Omega^2 + \delta^2}{4\Omega^2} \bar{n} + \frac{(\Omega - \delta)^2}{4\Omega^2} \right] \mathcal{D}_{\Sigma_+} \\ & + \gamma \frac{g^2}{4\Omega^2} (2\bar{n} + 1) \mathcal{D}_{\Sigma_z}, \end{aligned} \quad (33)$$

which corresponds to the FME if we make the approximations $\Gamma(\omega_j) = \gamma$, $N(|\omega_j|) \simeq \bar{n}$ which are accurate in the common regime of validity between OBE and FME.

As in this regime the FME is a time average of the OBE, it cannot yield more information about the dynamics. On the contrary, this coarse-graining seems to average out quantum properties of the dynamics that are captured by the OBE like the coherent nature of the energy exchange between the driving field and the atom. A similar procedure would allow us to derive the FME from the GBE Eq. (26), leading to master equation similar to Eq. (33), but which takes into account the frequency dependence of the mode thermal occupation. Once again, one can conclude that the FME do not bring more information than the GBE about the atomic dynamics for the range of parameters where both are valid. Finally, in the present context, the FME turns out to be really advantageous solely in the case of a reservoir correlation time of the order or larger than a single Rabi oscillation, for instance in the presence of a structured environment [24, 25], or for extremely low temperatures $T \lesssim \hbar\Omega/k_B$. The various conditions of validity of FME, OBE and GBE are summarized in Table I.

We have computed the expressions of the main dynamical quantities corresponding to the steady state of the FME and the OBE in their common regime of validity (Appendix B). The populations and coherences in the basis $\{|e\rangle, |g\rangle\}$ are plotted in Fig. 4 showing a very good agreement in the common domain of validity. The deviations between the two predicted steady states (and in particular the imaginary part of coherences which is non zero for OBE and strictly zero for FME) can be shown explicitly to vanish in the limit $\gamma/g \rightarrow 0$, $\hbar\Omega/k_B T \rightarrow 0$ and $|\delta|/\omega_L \rightarrow 0$, which are three conditions assumed in the

derivation of either the FME or the OBE (see Appendix B). Finally, we observe deviations between the two approaches at large temperature such that $\bar{n} > 1$. These deviations can be explained noting that $\gamma\bar{n}$ is the typical evolution rate of the atomic density operator in the interaction picture for high temperatures (rather than γ), and therefore the validity of the derivation of the FME actually requires $\Omega \gg \gamma\bar{n}$ to have a small variation of the density operator of the atom during the coarse-graining time Δt_{FME} . While this fact does not affect the global agreement of both methods within the common regime of validity, it points out the interest of the OBE to describe moderate drives such that $\Omega \lesssim \gamma$, or $\Omega \lesssim \gamma\bar{n}$ which cannot be captured by the FME.

III. THERMODYNAMICS OF FLUORESCENCE

In the sections above we have provided rigorous derivations of the OBE and the FME, and unambiguously clarified their respective regimes of validity by using a microscopic description of the reservoir. We now exploit our framework to provide new insights on the thermodynamics of light-matter interaction.

Despite the OBE are known for a long time, there is no consensus on their thermodynamical interpretation. Indeed, the thermodynamic description of a driven quantum system \mathcal{S} coupled to a thermal reservoir is well known under the conditions that (i) the drive is adiabatic, in the sense that the typical time-scale of variation of the system's Hamiltonian $H_S(t)$ is much longer than the coarse-graining time Δt_{cg} needed to derive the master equation, and (ii) the coarse-graining time Δt_{cg} is sufficiently long to resolve all the transition frequencies in the spectrum of $H_S(t)$ (see Section II). The master equations then takes the form $\dot{\rho}_S(t) = -i[H_S(t), \rho] + \mathcal{L}_t[\rho_S]$, where the Lindbladian \mathcal{L}_t adapts every time-step Δt_{cg} to the Hamiltonian $H_S(t)$. In this limit, pioneer studies have found the flow of work provided by the drive, and heat exchanged with the thermal reservoir to be [26, 27]:

$$\dot{W}_{\text{adiab}}(t) = \text{Tr}\{\rho_S(t) d_t H_S(t)\} \quad (34)$$

$$\dot{Q}_{\text{adiab}}(t) = \text{Tr}\{\mathcal{L}_t[\rho_S(t)] H_S(t)\}. \quad (35)$$

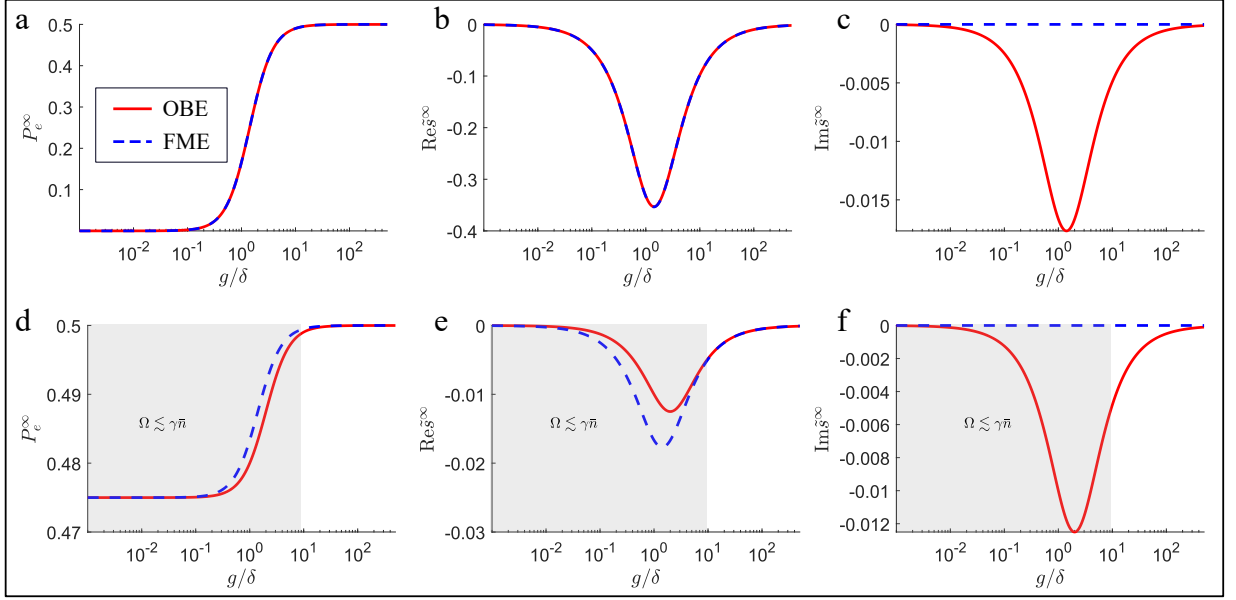


FIG. 4. Comparison of steady state values of the population (a,d) and the real (b,e) and imaginary (c,f) part of the amplitude of the coherences in the bare atomic basis, in the rotating frame, for the OBE (red solid) and FME (blue dashed). Parameters: $\delta/\omega_L = 1 \cdot 10^{-3}$, $\gamma/\omega_L = 1 \cdot 10^{-4}$, $\hbar\omega_L/k_B T = 10$ (a, b, c), $\hbar\omega_L/k_B T = 0.1$ (d, e, f). The grey area corresponds to values of g/δ such that $\Omega \lesssim \gamma\bar{n}$ and therefore the FME is expected not to be valid anymore.

This identification is validated by the proof of the positivity of the entropy production (second law) $\sigma = \Delta S - Q_{\text{adiab}}(t)/T$, which is based on Spohn's inequality [6, 28] $\dot{\sigma} = -k_B \text{Tr}\{\mathcal{L}_t[\rho_S(t)](\log \rho_S(t) - \log \pi_S(t))\} \geq 0$, where $\pi_S(t) = e^{-H_S(t)/k_B T}/Z_S$ is the instantaneous fixed point of \mathcal{L}_t .

Conversely, in the case under study, the characteristic time of variation of $H(t)$ is ω_L^{-1} which is much shorter than Δt_{cg} , such that these results cannot be applied directly. It was already shown in some cases going beyond the assumptions of Ref. [27] that correct splitting between work and heat requires more care, e.g. in the case of local Lindblad equations, one needs to specify the underlying microscopic model [5]. Similarly, studies based on the FME have used different techniques to infer [7, 10] or derive [8, 9] the heat flow and check its compatibility with the second law, and the found expression differs notably from the adiabatic expression Eq. (35).

Here, we will adopt the definition of the heat as being the energy provided by the thermal reservoir, in the line of classical stochastic thermodynamics. Such definition was shown to ensure the second law of thermodynamics provided the system and reservoir evolve through a global unitary [11]. Using the insights brought by the microscopic derivation of the OBE and the FME we presented in Section II, we will compute its expression, for the current microscopic model, and with a level of approximation consistent with the dynamics in each case. This way, we will both retrieve earlier results for the FME and establish a consistent thermodynamic description of the OBE.

Note that above and in the remainder of this article, we use when dealing with variations of thermodynamic quantities the notation d_t for time-derivative of state-variables, like the internal energy $U(t) = \text{Tr}\{\rho(t)H(t)\}$ or the Von Neumann entropy $S(t) = -k_B \text{Tr}\{\rho(t) \log \rho(t)\}$ of the atom, and the dot for the rates associated with path-dependent variables like the heat, work or entropy production.

A. Definition of the heat and proof of the second law

Before coming to our results, we briefly recall the approach of Ref. [11] when applied to the evolution between t and $t + \Delta t_{\text{cg}}$ of the driven atom. The key idea is to use the properties of the unitary operator $\mathcal{V}_{\Delta t_{\text{cg}}}$ dictating the evolution of the joint atom-reservoir system. We assume that we have at time t a factorized state of the joint atom-reservoir system $\rho_{S\mathcal{R}}(t) = \rho(t) \otimes \rho_{\mathcal{R}}^{\text{eq}}$, which is transformed into $\rho_{S\mathcal{R}}(t + \Delta t_{\text{cg}}) = \mathcal{V}_{\Delta t_{\text{cg}}} \rho(t) \otimes \rho_{\mathcal{R}}^{\text{eq}} \mathcal{V}_{\Delta t_{\text{cg}}}^\dagger$. The reduced state $\rho(t + \Delta t_{\text{cg}})$ of the atom fulfills a Lindblad equation as established by the derivations of Section II (either OBE or FME depending on chosen the coarse-graining time).

We then define the heat increment between t and $t + \Delta t_{\text{cg}}$ as the negative variation of the energy $E_{\mathcal{R}}$ of the reservoir, namely:

$$\begin{aligned} \Delta t_{\text{cg}} \dot{Q}(t) &= -\Delta t_{\text{cg}} d_t E_{\mathcal{R}}(t) \\ &= \text{Tr}\{H_{\mathcal{R}}(\rho_{\mathcal{R}S}(t) - \rho_{\mathcal{R}S}(t + \Delta t_{\text{cg}}))\}. \end{aligned} \quad (36)$$

Besides, the entropy production between t and $t + \Delta t$ is defined as:

$$\Delta t_{\text{cg}} \dot{\sigma}(t) = \Delta t_{\text{cg}} \left(d_t S_{\text{VN}}(t) + \frac{d_t E_{\mathcal{R}}(t)}{T} \right). \quad (37)$$

We then prove that the Eq. (37) can be recast as:

$$k_B S(\rho_{S\mathcal{R}}(t + \Delta t_{\text{cg}}) || \rho(t + \Delta t_{\text{cg}}) \otimes \rho_{\mathcal{R}}^{\text{eq}}), \quad (38)$$

i.e in terms of a quantum relative entropy $S(\rho_1 || \rho_2) = k_B \text{Tr}\{\rho_1(\log \rho_1 - \log \rho_2)\}$ which ensures its positivity. The proof that Eq. (38) is indeed equal to $\Delta t_{\text{cg}} \dot{\sigma}(t)$ can be done by expanding the quantum relative entropy:

$$\begin{aligned} & S(\rho_{S\mathcal{R}}(t + \Delta t_{\text{cg}}) || \rho(t + \Delta t_{\text{cg}}) \otimes \rho_{\mathcal{R}}^{\text{eq}}) \\ &= \text{Tr}\{\rho_{S\mathcal{R}}(t + \Delta t_{\text{cg}}) \log \rho_{S\mathcal{R}}(t + \Delta t_{\text{cg}})\} \\ &\quad - \text{Tr}\{\rho_{S\mathcal{R}}(t + \Delta t_{\text{cg}}) \log(\rho(t + \Delta t_{\text{cg}}) \otimes \rho_{\mathcal{R}}^{\text{eq}})\} \\ &= -S(t) - S_{\mathcal{R}}(t) + S(t + \Delta t_{\text{cg}}) \\ &\quad + \text{Tr}\left\{\rho_{S\mathcal{R}}(t + \Delta t_{\text{cg}}) \left(\frac{H_{\mathcal{R}}}{T} + k_B \log Z_{\mathcal{R}} \right)\right\} \\ &= \Delta t_{\text{cg}} d_t S(t) + (k_B \log Z_{\mathcal{R}} - S_{\mathcal{R}}(t)) + \frac{E_{\mathcal{R}}(t + \Delta t_{\text{cg}})}{T} \\ &= \Delta t_{\text{cg}} \left(d_t S(t) + \frac{d_t E_{\mathcal{R}}(t)}{T} \right). \end{aligned} \quad (39)$$

To go to the second equality, we used that the Von Neumann entropy of $\rho_{S\mathcal{R}}$ is conserved during the unitary $\mathcal{V}_{\Delta t_{\text{cg}}}$, and therefore its value at $t + \Delta t_{\text{cg}}$ is equal to its initial value $S(t) + S_{\mathcal{R}}(t)$ where we have denoted $S_{\mathcal{R}}(t) = -k_B \text{Tr}\{\rho_{\mathcal{R}}^{\text{eq}} \log \rho_{\mathcal{R}}^{\text{eq}}\}$ the Von Neumann entropy of the reservoir. The last equality is obtained using $S_{\mathcal{R}}(t) = E_{\mathcal{R}}(t)/T + k_B \log Z_{\mathcal{R}}$. It is now enough to use the positivity of relative entropy to prove that:

$$\dot{\sigma}(t) = d_t S(t) - \frac{\dot{Q}(t)}{T} \geq 0. \quad (40)$$

This derivation is general in the sense we did not have to specify the details of the evolution. It will therefore be valid for both the OBE and the FME, provided we are able to compute in each case the energy change of the reservoir.

B. Heat flow exchanged with the reservoir

The key step towards the wanted thermodynamic description is then to compute this heat flow, within the approximations and assumptions leading to the FME and the OBE. Due to the trace taken over the reservoir subspace, the master equation (FME or OBE) only captures the evolution of the atom degrees of freedom and does not contain anymore the information about the energy changes occurring in the reservoir. To circumvent this difficulty, we use an explicit calculation of the energy change of the reservoir which exploits the same techniques and approximations used to derive the FME and OBE in the previous section. This method is related to

the full counting statistics approach [29] which was used to derive the energy change of the reservoir in the case of the FME [9].

The first step of our derivation consists in inserting the reservoir Hamiltonian $H_{\mathcal{R}}$ in Eq. (11) inside the trace over the reservoir subspace, and take the trace over the system. This leads to a formal expression for the energy variation of the reservoir:

$$\begin{aligned} d_t E_{\mathcal{R}}(t) &= -\frac{1}{\hbar^2 \Delta t_{\text{cg}}} \int_t^{t+\Delta t_{\text{cg}}} dt' \int_t^{t'} dt'' \\ &\quad \text{Tr}_{\mathcal{R}} \left\{ H_{\mathcal{R}} [H_{\mathcal{R}S}^I(t'), [H_{\mathcal{R}S}^I(t''), \rho^I(t) \otimes \rho_{\mathcal{R}}^I]] \right\}. \end{aligned} \quad (41)$$

We then apply to Eq.(41) the same procedure used to derive the FME and OBE. Namely, we change the variable t'' to $\tau = t' - t''$, extend the upper limit of the integral over τ to $+\infty$ and use the explicit form of $H_{S\mathcal{R}}^I(t)$, obtaining:

$$\begin{aligned} d_t E_{\mathcal{R}}(t) &= \frac{1}{4\Delta t_{\text{cg}}} \int_t^{t+\Delta t_{\text{cg}}} dt' \sum_{l'} \sum_{\omega, \omega'} e^{i(\omega - \omega')t' + i(l-l')\omega_L t'} \\ &\quad \times A(-\omega - l\omega_L) \langle \tilde{\sigma}_l^\dagger(\omega') \tilde{\sigma}_l(\omega) \rangle + \text{c.c.}, \end{aligned} \quad (42)$$

where we introduced

$$A(\nu) = (1/\hbar^2) \int_{-\infty}^{\infty} d\tau e^{i\nu\tau} \langle [R^I(\tau), H_{\mathcal{R}}] R^I(0) \rangle. \quad (43)$$

The imaginary part of $\int_0^\infty d\tau e^{i\nu\tau} \langle [R^I(0), H_{\mathcal{R}}] R^I(\tau) \rangle$ is a contribution of similar order and form as the Lamb shift. We therefore neglect it to be consistent with the dynamical description. We then insert the explicit expression of R and $H_{\mathcal{R}}$ to obtain

$$A(\nu) = \hbar \nu G(\nu). \quad (44)$$

Eqs.(42)-(44) are essential to build our thermodynamical analysis.

The last step of the derivation is the Secular Approximation. As for the dynamics, two choices are possible, involving the coarse-graining times Δt_{FME} and Δt_{OBE} introduced in Section II A, leading to two different expressions for the heat flow consistent with the FME and the OBE, respectively. We treat the two cases below and give each time the expression of the first and second laws of thermodynamics.

C. Thermodynamics of the FME

Choosing $\Delta t_{\text{cg}} \equiv \Delta t_{\text{FME}}$ verifying Eq. (14) leads to neglect the terms with $l \neq l'$ and $\omega \neq \omega'$ in Eq. (42), yielding:

$$d_t E_{\mathcal{R}}(t) = \frac{1}{4} \sum_{l, \omega} A(-\omega - l\omega_L) \langle \sigma_l^\dagger(\omega) \sigma_l(\omega) \rangle + \text{c.c.} \quad (45)$$

Inserting Eq. (44) and defining the heat flow for the FME description as $\dot{Q}_{\text{FME}} = -d_t E_{\mathcal{R}}(t)$, we finally obtain:

$$\begin{aligned} \dot{Q}_{\text{FME}} = & -\sum_{j=1}^2 \hbar\omega_j (\gamma_{j,\downarrow} P_+(t) - \gamma_{j,\uparrow} P_-(t)) \\ & -\hbar\omega_L (\gamma_{0,\downarrow} - \gamma_{0,\uparrow}). \end{aligned} \quad (46)$$

This expression matches the heat flow in Refs. [7–10]. Using that the energy variation of the joint atom-reservoir system solely comes from the drive, one can deduce the work flow:

$$\begin{aligned} \dot{W}_{\text{FME}} = & \hbar\omega_L \left((\gamma_{1,\downarrow} - \gamma_{2,\downarrow}) P_+(t) - (\gamma_{1,\uparrow} - \gamma_{2,\uparrow}) P_-(t) \right. \\ & \left. + (\gamma_{0,\downarrow} - \gamma_{0,\uparrow}) \right). \end{aligned} \quad (47)$$

The first law of thermodynamics then reads $d_t U(t) = \dot{W}_{\text{FME}} + \dot{Q}_{\text{FME}}$.

We emphasize that the expressions Eqs. (46) and (47) are very different from their counterparts in the case of adiabatic (slow driving) master equations of Ref. [27]. In particular, we have that $\dot{W}_{\text{FME}} \neq \text{Tr}\{\dot{H}(t)\rho(t)\}$. The interpretation of these expressions is however clear when recalling that the FME describes reservoir-induced transitions that are assisted by the driving field which can take or provide a quantum of energy $\hbar\omega_L$ (see Section II B 1). From this picture, it appears that the work mechanism at play matches the classical thermodynamic notion of work of a non-conservative force. Indeed, the exchange of photons between the atom and driving field is included explicitly in the description when modeling the field by a cavity mode treated quantum-mechanically (see Section II B 1 and chapter 6 of Ref. [1]). The partial trace over the state of the field allowing to retrieve the FME from such description therefore reduces a pseudo-periodic problem – the infinite ladder of the field-atom energy diagram – onto an effective periodic description in a smaller configuration space – the two dressed states of the atom. Such reduction procedure is known in classical thermodynamics context to introduce non-conservative forces [30–33], associated with an energy flow that must be accounted as work despite its apparent dissipative nature. Here, this energy flow simply accounts for the variation of the field photon number associated with each transition. The constant term proportional to $\hbar\omega_L$ in the heat flow (last line of Eq. (46)) can be seen as another witness of this so-called radiative cascade [1] obtained when the field-atom system decays along the infinite ladder of their energy diagram. Indeed, it comes from the so-called “pseudo-transitions” [8], i.e. the transitions $|+(n_L)\rangle \rightarrow |+(n_L \pm 1)\rangle$ and $|-(n_L)\rangle \rightarrow |-(n_L \pm 1)\rangle$, which in the reduced two-level description only result in a pure dephasing-rate with no apparent change of populations, but as it is clear in the cavity-atom space are associated with a transfer of energy from the driving field directly into the reservoir.

Remarkably, the second law appears in the case of the FME as a consequence of the Spohn inequality, just as

for the adiabatic master equations. If one introduces the fixed points $\pi_j = \exp(-\hbar\omega_j \Sigma_z / k_B T) / Z_j$ of the dissipation superoperators \mathcal{L}_j for $j = 1, 2$ where Z_j are the corresponding partition functions, the entropy production rate reads:

$$\begin{aligned} \dot{\sigma}_{\text{FME}} = & d_t S_{\text{VN}} - \frac{\dot{Q}_{\text{FME}}(t)}{T} \\ = & -\sum_{j=1}^2 \text{Tr}\{\mathcal{L}_j[\rho(t)] (\log \rho(t) - \log \pi_j)\} \\ & + \frac{\hbar\omega_L}{T} \frac{g^2}{4\Omega^2} \Gamma(\omega_L) \geq 0. \end{aligned} \quad (48)$$

The first line is positive due to the Spohn inequality [6, 27, 28]. The second line corresponds to the contribution of the “pseudo-transitions” mentioned above, which is always positive.

As mentioned earlier, the drive does not induce coherences in the dressed basis, and the FME prepares a state diagonal in the basis $\{|+\rangle, |-\rangle\}$. Consequently, as soon as the coherences initially present are dissipated, i.e. after a typical time $\sim [\sum_j (\gamma_{j,\uparrow} + \gamma_{j,\downarrow})]^{-1}$, the quantity $\dot{\sigma}_{\text{FME}}$ resembles the entropy production of a *classical* two-level atom (described by a state always diagonal in the dressed basis $\{|+\rangle, |-\rangle\}$) in contact with two thermal reservoirs of effective temperatures $k_B T_j = \hbar\Omega / \log(\gamma_{j,\downarrow}/\gamma_{j,\uparrow})$, $j = 1, 2$. The only difference is the constant positive term $\frac{\hbar\omega_L}{T} \frac{g^2}{4\Omega^2} \Gamma(\omega_L)$ coming from the “pseudo-transitions”.

Remarkably, as a consequence of the long coarse-graining procedure, the unitary process associated with the periodic drive has been mixed with the dissipation happening in the reservoir. In this description, the coherent nature of the energy transfer between the driving field and the atom is therefore hidden, and the qubit’s stationary state differs from thermal equilibrium in the dressed state basis solely because of the value of its populations. The non-thermal nature of the driving is solely manifested in the fact that the effective thermal channel 2 has a negative temperature $T_2 = -\Omega T / \omega_2$, which results in a non-conservative force associated with the work flow \dot{W}_{FME} . This property does not rely on any quantum effect and can be emulated classically.

This motivates the analysis of the thermodynamic description associated with the OBE, involving a shorter coarse-graining time allowing clear separation of the actions of the driving and the reservoir, and the observation of coherent energy transfers with the driving field.

D. Thermodynamics of the OBE

We now choose $\Delta t_{\text{cg}} = \Delta t_{\text{OBE}}$ and neglect the terms with $l \neq l'$ in Eq. (42) while keeping the terms $\omega \neq \omega'$. We also use the flat spectrum assumption used to derive the OBE, which amounts to the replacement $A(-\omega - l\omega_L) \simeq -l(\omega + l\omega_L)G(-l\omega_L)$. Computing the integration

over t' up to first order in $\Omega\Delta t_{cg} \ll 1$ leads to the final expression:

$$\begin{aligned} d_t E_{\mathcal{R}}(t) &= \sum_{\omega, l} \hbar(\omega - l\omega_L) G(-l\omega_L) \text{Re} \langle \tilde{\sigma}_l^\dagger \tilde{\sigma}_l(\omega) \rangle \\ &= \gamma \sum_{\omega} \hbar(\omega + \omega_L)(\bar{n} + 1) \text{Re} \langle \tilde{\sigma}_+ \tilde{\sigma}_-(\omega) \rangle + \\ &\quad -\gamma \sum_{\omega} \hbar(\omega - \omega_L) \bar{n} \text{Re} \langle \tilde{\sigma}_- \tilde{\sigma}_+(\omega) \rangle \\ &= \gamma \hbar \omega_0 \left((\bar{n} + 1) P_e(t) - \bar{n} P_g(t) \right) + \gamma \hbar g \frac{2\bar{n} + 1}{2} \text{Re} \tilde{s}(t). \end{aligned}$$

It is then straightforward to prove:

$$\begin{aligned} \dot{Q}(t) &= -d_t E_{\mathcal{R}}(t) \\ &= \text{Tr} \{ H(t) \mathcal{L}_{\text{OBE}}[\rho(t)] \}. \end{aligned} \quad (49)$$

Using as before energy conservation between the reservoir and the atom, we obtain the expression of the work:

$$\begin{aligned} \dot{W}(t) &= -\hbar \omega_L \text{Im} \tilde{s}(t) \\ &= \text{Tr} \{ \rho(t) d_t H(t) \}, \end{aligned} \quad (50)$$

and the first law reads $d_t U(t) = \dot{W}(t) + \dot{Q}(t)$. Therefore, in sharp contrast with the case of the FME, the work and heat flow for the OBE have an expression similar to the case of an adiabatic driving [27]. Interestingly, one cannot link in this case $\dot{Q}(t)$ to the thermal equilibrium state, i.e. $\dot{Q}(t) \neq -\text{Tr} \{ \mathcal{L}_{\text{OBE}}[\rho(t)] \log \pi \}$, where $\pi = e^{-H_0/k_B T}/Z$ is the fixed point of the Lindbladian \mathcal{L}_{OBE} . Consequently, one *cannot* use Spohn's inequality to prove the positivity of the entropy production rate:

$$\dot{\sigma} = d_t S_{\text{VN}}(t) - \frac{\dot{Q}(t)}{T}. \quad (51)$$

However, the result of section III A applies and ensures that Eq. (51) satisfies the second law $\dot{\sigma} \geq 0$. Eqs. (49)-(51) are the main new results of our thermodynamic analysis.

These differences (form of the heat flow and impossibility to use the Spohn inequality) with respect to the thermodynamic description of adiabatic master equations and the FME are ultimately the consequences of the structure of the OBE which cannot be reduced in any basis to a classical-like rate equation.

As a supplementary check of the consistency of our results, we compare the steady-state heat and work flow derived for the OBE from those obtained in Ref. [7, 8, 10] working with the FME, given by Eqs. (46)-(47). As before, we work in the common regime of validity between the OBE and the FME, as captured by Eq. (67). Fig. 5 shows the excellent agreement between the approaches. As for the dynamics, we find evidence of the requirement $\Omega \gg \gamma \bar{n}$ for the FME to be valid.

IV. QUANTUM SIGNATURES IN THE THERMODYNAMIC OF FLUORESCENCE

In Sections I and II, we have built a consistent thermodynamical framework for the OBE, able to capture

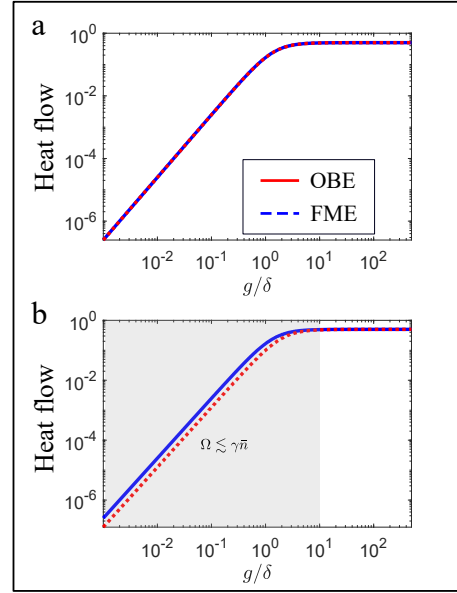


FIG. 5. Comparison of steady state values of the heat flow for the OBE (red solid) and FME (blue dashed). Parameters: $\delta/\omega_L = 1 \cdot 10^{-3}$, $\gamma/\omega_L = 1 \cdot 10^{-4}$, $\hbar\omega_L/k_B T = 10$ (a), $\hbar\omega_L/k_B T = 0.1$ (b). The gray area corresponds to values of g/δ such that $\Omega \lesssim \gamma \bar{n}$ and therefore the FME is expected not to be valid anymore.

the coherent regime of light matter interaction. In this last Section, we exploit this framework to single out a genuinely quantum non-equilibrium steady state, and evidence unambiguous quantum signatures in the thermodynamical quantities characterizing the resonance fluorescence.

A. Quantum Non-equilibrium steady state

In the classical realm, non-equilibrium steady states (NESS) are typically produced by coupling the system of interest to thermal baths of different temperatures, or by driving it in a non-adiabatic manner. Transposed in the quantum regime, the latter situation can generate genuinely quantum NESS characterized by the presence of steady state coherences in the energy basis of the bare system [34]. The present situation provides a canonical example of such quantum NESS. To make this obvious, it is convenient to study the atomic evolution in the Bloch sphere in the frame rotating at the drive frequency. The atom dynamics is governed by the effective Hamiltonian \tilde{H}_{eff} , while the Lindbladian remains unchanged. The average population of the excited (ground) state $P_e(t) = \langle e | \tilde{\rho}(t) | e \rangle = \langle e | \rho(t) | e \rangle$ ($P_g(t) = \langle g | \rho(t) | g \rangle$) and the average dipole $\tilde{s}(t) = \langle e | \tilde{\rho}(t) | g \rangle = e^{i\omega_L t} \langle e | \rho(t) | g \rangle$

obey the following evolution equations:

$$\dot{P}_e(t) = -\gamma((\bar{n} + 1)P_e(t) - \bar{n}P_g(t)) + \frac{ig}{2}(\tilde{s}(t) - \tilde{s}(t)^*) \quad (52a)$$

$$\dot{\tilde{s}} = -\left(i\delta + \frac{\gamma(2\bar{n} + 1)}{2}\right)\tilde{s}(t) + ig\left(P_e(t) - \frac{1}{2}\right). \quad (52b)$$

These equations captures oscillations of the population of the excited state at frequency Ω induced by the drive. These oscillations are associated with coherence periodically building up in the bare atomic basis $\{|e\rangle, |g\rangle\}$ as quantified by $\tilde{s}(t)$ becoming non-zero. In addition, the reservoir induces dephasing in basis $\{|e\rangle, |g\rangle\}$. The competition between these effects result in a genuinely quantum non-equilibrium dynamics, that is a direct consequence from the fact that the eigenbasis of the effective Hamiltonian does not commute with the eigenbasis of the thermal equilibrium state π . Therefore the steady state $\tilde{\rho}_{\text{OBE}}^\infty$ of Eq. (52) is in general different from the thermal equilibrium state π and may carry coherences in the bare atom energy eigenbasis, defining a quantum non-equilibrium steady state (see Eq. (68) in the Appendix B for the detailed expression).

In quantum thermodynamics, the non-equilibrium nature of a given state can be related to its so-called quantum relative entropy to the equilibrium state. Precisely, the relative entropy between two quantum states ρ_1 and ρ_2 is defined as $D[\rho_1||\rho_2] = \text{Tr}[\rho_1(\log(\rho_1) - \log(\rho_2))]$. In the present situation, the relative entropy between the steady state $\tilde{\rho}^\infty$ and the thermal equilibrium π splits into two components, giving rise to two non-equilibrium features:

$$D[\tilde{\rho}_{\text{OBE}}^\infty||\pi] = D_q + D_d \quad (53)$$

$$D_q = D[\tilde{\rho}_{\text{OBE}}^\infty||\rho_d^\infty] \quad (54)$$

$$D_d = D[\rho_d^\infty||\pi]. \quad (55)$$

We have introduced $\rho_d^\infty = \sum_{i=e,g} |i\rangle\langle i|\tilde{\rho}_{\text{OBE}}^\infty|i\rangle\langle i|$ the projection of the steady state on the z axis of the Bloch sphere. A strictly positive value of D_d signals that the steady state populations are different from the thermal ones, which characterizes a classical NESS. On the other hand, steady state coherences in the bare atom energy eigenbasis define a genuinely quantum NESS highlighted by a strictly positive D_q .

We have plotted in Fig. 6a (resp. b) the behavior of D_d (resp. D_q) as a function of the driving strength g and detuning δ for a fixed temperature $T = \hbar\omega_L/2k_B$. As it appears in the Figure, equilibrium (resp. classical NESS) is typically reached as soon as $g \leq \gamma$ or $g \leq \delta$ (resp. for the opposite conditions). The boundary regions defined by the conditions (i) $\gamma \sim g \geq \delta$ or (ii) $g \sim \delta \geq \gamma$ gives rise to two distinct situations of quantum NESS. The resonant regime (i) is governed by the damping: It induces a delay between the atomic dipole and the drive evolution and purely imaginary coherences $\text{Im}\tilde{s}^\infty$. Conversely, in the detuned regime (ii) the damping is negligible such

that the eigenstates of $\tilde{\rho}_{\text{OBE}}^\infty$ become aligned with the eigenstates of the effective Hamiltonian \tilde{H}_{eff} where the dipole coherences are purely real. As it appears in the Figure, the quantum NESS is fragile and vanishes as soon as the driving strength becomes too weak ($\delta, \gamma \geq g$) or too strong ($g \geq \gamma, \delta$).

B. The role of coherences in the energy balance

One can find a correspondance to these features in the first law. We first focus on the internal energy of the atom $U(t) = \text{Tr}\{\rho(t)H(t)\}$, which can be rewritten $U(t) = U_d(t) + U_q(t)$, where $U_d(t) = \hbar\omega_0/2\langle\sigma_z\rangle$ and $U_q(t) = \hbar g \text{Re}\tilde{s}(t)$. U_d is the component of energy acquired by the driven atom, that is stored in the populations. Conversely, U_q is a genuinely quantum energetic component that is stored in the atomic coherences, namely in the atomic dipole that is phase-tuned with the driving field: It constitutes our first quantum thermodynamical signature. Its physical meaning clearly appears when considering the quantum evolution of the system composed of the atom and a single cavity modetaken as a quantum mechanical model of the driving field (i.e. the radiative cascade picture mentioned earlier). The Jaynes Cummings Hamiltonian describing the interaction between this cavity mode and the atom induces periodic exchanges of a quantum of energy between the atom and the field (Rabi oscillation). The energetic component $U_q(t)$ is necessary so that energy and particle number conservation are compatible when the atom and the drive are detuned: It thus oscillates in phase with the Rabi oscillations, has the same sign as the detuning δ , and vanishes at resonance (see Appendix C).

One can find another quantum thermodynamic signature by splitting heat flow into two contributions:

$$\dot{Q}(t) = \dot{Q}_{\text{cl}}(t) + \dot{Q}_q(t), \quad (56)$$

where:

$$\begin{aligned} \dot{Q}_{\text{cl}}(t) &= \text{Tr}\{\mathcal{L}_{\text{OBE}}[\rho]H_0\} \\ &= -\gamma\hbar\omega_0[(\bar{n} + 1)P_e(t) - \bar{n}p_g(t)] \end{aligned} \quad (57)$$

can be understood as the total heat flow for a classical two-level system of energy splitting $\hbar\omega_0$ and which cannot be prepared in a superposition of its two energy eigenstates. $Q_{\text{cl}}(t)$ vanishes at thermal equilibrium and is non zero in the classical NESS region (see Fig. (6)c). On the other hand, the quantity

$$\dot{Q}_q(t) = \text{Tr}\{\mathcal{L}_{\text{OBE}}[\rho]V(t)\} \quad (58)$$

$$= -\gamma\hbar g \frac{2\bar{n} + 1}{2} \text{Re}\tilde{s}(t), \quad (59)$$

is non-zero only in presence of coherences induced by the drive in the free qubit energy eigenbasis $\{|e\rangle, |g\rangle\}$, i.e. in the case of a quantum NESS (see Fig. 6d). From Eq. (58),

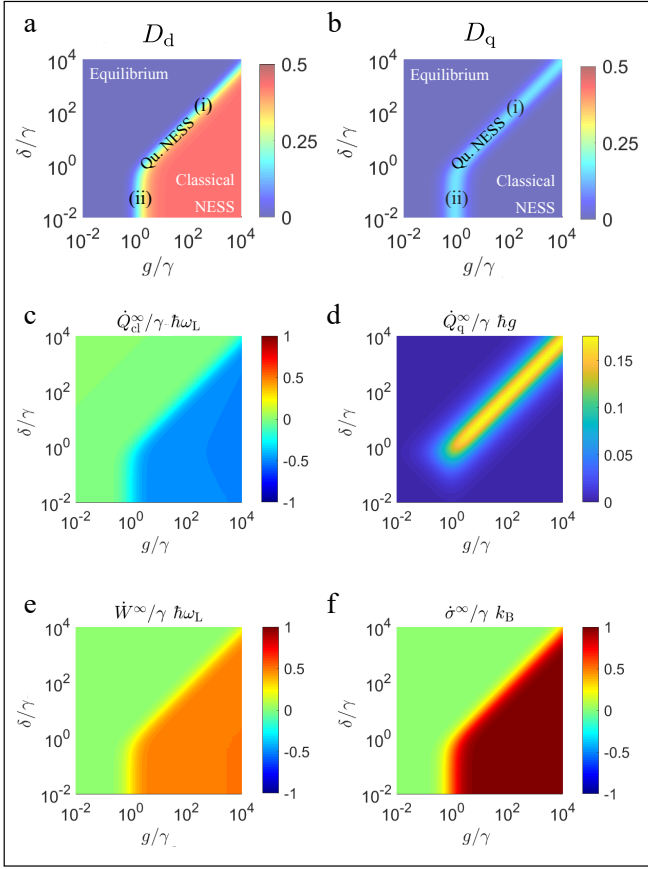


FIG. 6. Quantum signatures in the steady state and thermodynamics of the OBE. **a**: Entropic distance D_d , defined in Eq. (55), between the projection ρ_d^∞ of the steady state $\tilde{\rho}_{\text{OBE}}^\infty$ on the z -axis and the thermal equilibrium state π . **b**: Entropic distance D_q , defined in Eq. (54), between the steady state $\tilde{\rho}_{\text{OBE}}^\infty$ and ρ_d^∞ . **c**: Classical contribution $\dot{Q}_{\text{cl}}^\infty$ of the steady state heat flow. **d**: Quantum contribution $\dot{Q}_{\text{q}}^\infty$ of the steady state heat flow. **e**: Steady state work flow \dot{W}^∞ . **f**: Steady state entropy production σ^∞ .

one can interpret the term $\dot{Q}_{\text{q}}(t)$ as the variation of U_{q} induced by the thermal reservoir – in other words, the energy cost for the reservoir to erase the coherences in the $\{|e\rangle, |g\rangle\}$ basis.

Because the steady state of the OBE exhibits non-zero coherences, the stationary quantum contribution to heat is non-zero and takes the value:

$$\dot{Q}_{\text{q}}^\infty = \frac{\gamma}{2} \frac{\hbar \delta}{1 + 2 \frac{\delta^2}{g^2} + \frac{\gamma^2 (2\bar{n} + 1)^2}{2g^2}}. \quad (60)$$

The quantity $\dot{Q}_{\text{q}}^\infty$ has the sign of the detuning δ , such that the entropy production in presence of coherences is smaller (resp. larger) than in the absence of coherences when the detuning is positive (resp. negative). This reflects the fact that the energy stored in the interaction between the atom and the driving field can be either pos-

itive (repulsive interaction) or negative (attractive interaction), such that erasing the coherences may either cost or provide energy to the reservoir (see Appendix C).

The work flow and the entropy production are plotted in Fig. 6e and f, respectively. From Fig. 6, it is clear that the quantum heat is non zero solely when D_q is non-zero, in the quantum NES of type (ii) as defined in Section IV A, i.e. when $g \sim \delta \geq \gamma$. On the other hand, the both quantum and classical NES give rise to finite work and classical heat flows, and therefore a non zero-entropy production.

V. CONCLUSION

We have shown that despite their “local” nature, the optical Bloch equations (OBE) are fully compatible with thermodynamics and can be used to derive a first and second law of thermodynamics. Our results are based on a partial secular approximation and evidence that OBE accurately describe the coupling of a driven two-level atom to a reservoir at thermal equilibrium for a large range of parameters. Interestingly, we even found that the Floquet master equation used so far to study thermodynamics of fluorescence can be derived from the OBE via a time coarse-graining. Building on our description, we computed the heat flow defined as the power received from the reservoir to show the OBE comply with the second law of thermodynamics. Surprisingly, we find that the expressions of the work and heat flows take the same form as in the case of an adiabatic master equation (slowly varying Hamiltonian), even though the OBE are far outside this regime. Finally, we highlighted that the OBE allow to investigate shorter time-scale than Floquet-based approach, corresponding to a fraction of a Rabi oscillation, on which quantum effect associated with the coherent nature of the driving can be observed. We have identified in the heat flow the contribution depending on coherences in the bare atom energy eigenbasis which signals this quantum regime. Our work bridges the gap between thermodynamics and quantum optics, and therefore brings within reach important applications such that the energetics of quantum computation.

Acknowledgements We thank Gregory Bulnes Cuetara for enlightening discussions. Work by C.E. was supported by the US Department of Energy (DOE), Office of Sciences, Basic Energy Sciences (BES), under Award No. DE-SC0017890. M.E. is funded by the European Research Council (project NanoThermo, ERC-2015-CoG Agreement No. 681456). This work was conducted in part at the KITP, a facility supported by the U.S. National Science Foundation under Grant No. NSF PHY-1748958.

APPENDIX A: LAMB AND LIGHT SHIFTS

The master equation Eq. (11), once $H_{\mathcal{SR}}^I(t)$ was replaced with its explicit expression contains term involving the quantity

$$K(\nu) = \frac{1}{\hbar^2} \int_0^\infty d\tau e^{i\nu\tau} \langle R^I(\tau) R^I(0) \rangle, \quad (61)$$

whose real part $\text{Re}K(\nu) \equiv G(\nu)/2$ is the spectral density defined in Eq.(6). This identity uses that the correlation function is invariant under time translation:

$$\begin{aligned} \langle R^I(t+\tau) R^I(t) \rangle &= \sum_k g_k^2 \left[e^{-i\omega_k\tau} N(\omega_k) \right. \\ &\quad \left. + e^{i\omega_k\tau} (N(\omega_k) + 1) \right] \\ &= \langle R^I(\tau) R^I(0) \rangle. \end{aligned} \quad (62)$$

The imaginary part

$$\begin{aligned} D(\nu) &= 2\text{Im}K(\nu) \\ &= 2\mathcal{P} \sum_k g_k^2 \left[\frac{N(\omega_k)}{\nu - \omega_k} + \frac{N(\omega_k) + 1}{\nu + \omega_k} \right], \end{aligned} \quad (63)$$

where \mathcal{P} stands for the Cauchy principal value, contributes to $\dot{\rho}$ with a term:

$$\begin{aligned} \dot{\rho}_{\text{sh.}} &= \frac{i}{4} \sum_\omega D(-\omega + \omega_L) (\sigma_-(\omega) \rho \sigma_+ - \sigma_+ \sigma_-(\omega) \rho - \text{h.c.}) \\ &+ \frac{i}{4} \sum_\omega D(-\omega - \omega_L) (\sigma_+(\omega) \rho \sigma_- - \sigma_- \sigma_+(\omega) \rho - \text{h.c.}). \end{aligned} \quad (64)$$

Using that $\Omega \ll \omega_L$ and neglecting the dependence of the system-reservoir coupling and thermal occupation function on ω as in Section II C, we obtain:

$$\dot{\rho}_{\text{sh.}} \simeq -\frac{i}{4} D(\omega_L) [\sigma_+ \sigma_-, \rho] - \frac{i}{4} D(-\omega_L) [\sigma_- \sigma_+, \rho]. \quad (65)$$

This contribution can be interpreted as a renormalization of the atomic transition frequency by an amount:

$$\delta_{\text{sh.}} = \frac{D(\omega_L) - D(-\omega_L)}{2}. \quad (66)$$

This value accounts both for the Lamb shift (value for $\bar{n} = 0$) and the dynamic Stark shift, or light shift (temperature dependent part). Values of these shifts are computed in Ref.[16] for typical Rydberg atoms, finding typical values in the kHz range on top of GHz transitions.

APPENDIX B: FME VS OBE, STEADY STATE COMPARISON

Characterization of the steady state

The two master equations corresponding to the OBE and FME have very different forms and different conditions of validity. However, it exists a regime of parameters such that both choices of coarse-grainings are valid,

which is:

$$\omega_0, \omega_L, \tau_c^{-1} \gg \Omega \gg \gamma. \quad (67)$$

Provided that $G(\nu)$ is flat around frequencies $\pm\omega_0$, both the FME and the OBE are therefore expected to be valid for parameters complying with Ineq.(67).

In order to compare the predictions of both methods, we look at the steady-state values of the population of the excited state $P_e = \langle e | \tilde{\rho}^\infty | e \rangle$ and of the coherence amplitude $\tilde{s} = \langle e | \tilde{\rho}^\infty | g \rangle$. For the OBE, we get:

$$P_e^\infty = \frac{1}{2\bar{n} + 1} \left(\bar{n} + \frac{1/2}{1 + 2\frac{\delta^2}{g^2} + \frac{\gamma^2(2\bar{n} + 1)^2}{2g^2}} \right) \quad (68a)$$

$$\tilde{s}^\infty = -\frac{\frac{\delta}{g(2\bar{n} + 1)} + i\frac{\gamma}{2g}}{1 + 2\frac{\delta^2}{g^2} + \frac{\gamma^2(2\bar{n} + 1)^2}{2g^2}}, \quad (68b)$$

while we use the definitions of the dressed states Eqs.(4a)-(4b) to deduce that in the case of the FME:

$$P_e^\infty = \frac{1}{2} + \frac{\delta}{2\Omega} (2\tilde{P}_+^\infty - 1) \quad (69)$$

$$\tilde{s}^\infty = \frac{g}{2\Omega} (2\tilde{P}_+^\infty - 1), \quad (70)$$

where P_+^∞ is given in Eq. (24).

Deviation between the OBE and FME steady states in the common regime of validity

In order to assess analytically the correspondence between the steady state predicted by OBE and FME approach in the common regime of validity, we make an expansion of the difference between the expressions for the steady state values of P_e , $\text{Re}\tilde{s}$ and $\text{Im}\tilde{s}$ for small values of γ/g and $\hbar\Omega/k_B T$ and $|\delta|/\omega_L$. Denoting $\Delta X = X^{\text{FME}} - X^{\text{OBE}}$ for $X \equiv P_e$, $\text{Re}\tilde{s}$ or $\text{Im}\tilde{s}$, we obtain up to first order in $\frac{\gamma}{g}$, $\frac{\hbar\Omega}{k_B T}$ and $\frac{\hbar\omega_L}{k_B T}$:

$$\Delta P_e \simeq \frac{\delta}{\omega_L} \frac{2e^{\frac{\hbar\omega_L}{k_B T}} \frac{\hbar\omega_L}{k_B T}}{(1 + e^{\hbar\omega_L/k_B T})^2} \frac{\delta^2}{g^2 + 2\delta^2} \quad (71)$$

$$\Delta \text{Re}\tilde{s} \simeq \frac{\delta}{\omega_L} \frac{\frac{\hbar\omega_L}{k_B T}}{1 + \cosh(\frac{\hbar\omega_L}{k_B T})} \frac{g\delta}{g^2 + 2\delta^2} \quad (72)$$

$$\Delta \text{Im}\tilde{s} \simeq \frac{\gamma}{2g} \frac{g^2}{g^2 + 2\delta^2}. \quad (73)$$

Using

$$\frac{\delta^2}{g^2 + 2\delta^2}, \quad \frac{\delta g}{g^2 + 2\delta^2}, \quad \frac{g^2}{g^2 + 2\delta^2} \leq 1 \quad (74)$$

and

$$\frac{2e^{\frac{\hbar\omega_L}{k_B T}} \frac{\hbar\omega_L}{k_B T}}{(1 + e^{\hbar\omega_L/k_B T})^2}, \quad \frac{\frac{\hbar\omega_L}{k_B T}}{1 + \cosh(\frac{\hbar\omega_L}{k_B T})} \leq \frac{1}{2}, \quad (75)$$

it is straightforward to conclude that in the the discrepancy between OBE and FME steady state values is negligible in the limit where γ/g , $\hbar\Omega/k_B T$ and $|\delta|/\omega_L$ go to zero, which are three conditions required to have both FME and OBE descriptions to be valid.

APPENDIX C: TWO-LEVEL ATOM AND DRIVE AS A CLOSED SYSTEM

A. Model of the drive as a cavity field

To provide a physical interpretation of the dynamics captured by the FME and also to the quantum heat term, it is convenient to go beyond the classical approximation and model the laser as a coherent field $|\alpha\rangle$ injected in an effective cavity mode of frequency ω_L and containing a large number of photons $|\alpha|^2 \gg 1$ [1]. The complete Hamiltonian of the atom and the field reads

$$H_{af} = \frac{\hbar\omega_0}{2}\sigma_z + \frac{\hbar g_0}{2}(a^\dagger\sigma + \sigma^\dagger a) + \hbar\omega_L a^\dagger a \quad (76)$$

where a is the mode annihilation operator. The semi-classical description used in the main text is recovered by neglecting the action of the atom on the field, that freely evolve in time $|\alpha e^{-i\omega_L t}\rangle$. Tracing over the field mode gives an effective time-dependent Hamiltonian for the atom that matches $H(t)$.

B. Energy balance in presence of detuning

This model gives also an interesting interpretation of the quantum contribution to the heat flow. Starting from the product state $|g, \alpha\rangle$ the atom and the field get slowly and weakly entangled [?]. In the absence of coupling to the reservoir, the joint state at time t fulfills $|\Psi(t)\rangle = |e, \psi_e(t)\rangle + |g, \psi_g(t)\rangle$ where $|\psi_e(t)\rangle$ (resp. $|\psi_g(t)\rangle$) is the (not normalized) field state correlated with the atomic excited (resp. ground) state, verifying $\langle\psi_e|\psi_g\rangle \sim 1$. The population of the excited (resp. ground) state reads $P_e(t) = \langle\psi_e(t)|\psi_e(t)\rangle$ (resp. $P_g(t) = \langle\psi_g(t)|\psi_g(t)\rangle$) while the number of photons in the cavity reads $N(t) = \langle\psi(t)|a^\dagger a|\psi(t)\rangle$. Since the Hamiltonian conserves the number of excitations, we have $P_e(t) + N(t) = N(0) = |\alpha|^2$.

The global energy of the joint system reads $U_{\text{tot}} = U_d(t) + U_q(t) + \hbar\omega_L N(t)$ with $U_d(t) = \hbar\omega_0(P_e(t) + 1)/2$ and $U_q(t) = \hbar g_0 \text{Re}[\langle\alpha_e(t)|\alpha_g(t)\rangle]$. Here, $U_d(t)$ is the part of atomic internal energy stored in the population, while in the classical limit $U_q(t)$ becomes $U_q(t) = \hbar g \text{Re}[\tilde{s}(t)]$ where we have defined the classical Rabi frequency $g = g_0|\alpha|$: In the classical limit, $U_q(t)$ is thus the atomic energy component stored in the coherences. U_{tot} is conserved during the unitary evolution, such that $\hbar\omega_0 P_e(t) + \hbar\omega_L N(t) + U_q(t) = \omega_L N(0)$. Denoting as $\delta = \omega_0 - \omega_L$, we finally get

$$\hbar\delta P_e(t) + U_q(t) = 0 \quad (77)$$

$U_q(t)$ thus appears as the necessary energetic component that ensures the compatibility of the excitation number and energy conservation laws.

-
- [1] Cohen-Tannoudji, C., Dupont-Roc, J. & Grynberg, G. *AtomPhoton Interactions : Basic Process and Applications* (Wiley-VCH Verlag GmbH, Weinheim, Germany, 1998). URL <http://dx.doi.org/10.1002/9783527617197>.
 - [2] Levy, A. & Kosloff, R. The local approach to quantum transport may violate the second law of thermodynamics. *EPL* **107**, 20004 (2014).
 - [3] Hofer, P. P. *et al.* Markovian master equations for quantum thermal machines: local vs global approach. *arXiv* (2017). 1707.09211.
 - [4] González, J. O. *et al.* Testing the Validity of the ‘Local’ and ‘Global’ GKLS Master Equations on an Exactly Solvable Model. *Open Syst. Inf. Dyn.* **24**, 1740010 (2017).
 - [5] De Chiara, G. *et al.* Reconciliation of quantum local master equations with thermodynamics. *New J. Phys.* **20**, 113024 (2018).
 - [6] Breuer, H.-P. & Petruccione, F. *The Theory of Open Quantum Systems* (Oxford University Press, 2007). URL <http://dx.doi.org/10.1093/acprof:oso/9780199213900.001.0001>.
 - [7] Szczygielski, K., Klimovsky, D. G. & Alicki, R. Markovian master equation and thermodynamics of a two-level system in a strong laser field. *Phys. Rev. E* **87**, 012120+ (2013). URL <http://dx.doi.org/10.1103/physreve.87.012120>.
 - [8] Langemeyer, M. & Holthaus, M. Energy flow in periodic thermodynamics. *Physical Review E* **89**, 012101+ (2014). URL <http://dx.doi.org/10.1103/physreve.89.012101>.
 - [9] Cuetara, G. B., Engel, A. & Esposito, M. Stochastic thermodynamics of rapidly driven systems. *New Journal of Physics* **17**, 055002+ (2015). URL <http://dx.doi.org/10.1088/1367-2630/17/5/055002>.
 - [10] Donvil, B. Thermodynamics of a periodically driven qubit. *Journal of Statistical Mechanics: Theory and Experiment* **2018**, 043104+ (2018). URL <http://dx.doi.org/10.1088/1742-5468/aab857>.
 - [11] Esposito, M., Lindenberg, K. & Van den Broeck, C. Entropy production as correlation between system and reservoir. *New Journal of Physics* **12**, 013013+ (2010). URL <http://dx.doi.org/10.1088/1367-2630/12/1/013013>.
 - [12] Kubo, R. Statistical-Mechanical Theory of Irreversible Processes. I. General Theory and Simple Applications to Magnetic and Conduction Problems. *J. Phys. Soc. Jpn.* **12**, 570–586 (1957).
 - [13] Martin, P. C. & Schwinger, J. Theory of Many-Particle Systems. I. *Phys. Rev.* **115**, 1342–1373 (1959).
 - [14] Redfield, A. G. The Theory of Relaxation Processes.

- Adv. Magn. Opt. Reson.* **1**, 1–32 (1965).
- [15] Gaspard, P. & Nagaoka, M. Slippage of initial conditions for the Redfield master equation. *J. Chem. Phys.* **111**, 5668–5675 (1999).
 - [16] Farley, J. W. & Wing, W. H. Accurate calculation of dynamic Stark shifts and depopulation rates of Rydberg energy levels induced by blackbody radiation. Hydrogen, helium, and alkali-metal atoms. *Phys. Rev. A* **23**, 2397 (1981).
 - [17] Carmichael, H. *Statistical Methods in Quantum Optics 1: Master equations and Fokker-Planck equations* (Springer, 2002). URL <http://www.worldcat.org/isbn/3540548823>.
 - [18] Lindblad, G. On the generators of quantum dynamical semigroups. *Communications in Mathematical Physics* **48**, 119–130 (1976). URL <http://dx.doi.org/10.1007/bf01608499>.
 - [19] Davies, E. B. Markovian master equations. *Commun. Math. Phys.* **39**, 91–110 (1974). URL <https://projecteuclid.org/euclid.cmp/1103860160>.
 - [20] Mollow, B. R. Power spectrum of light scattered by two-level systems. *Physical Review* **188**, 1969–1975 (1969). URL <http://dx.doi.org/10.1103/physrev.188.1969>.
 - [21] Alicki, R., Lidar, D. A. & Zanardi, P. Internal consistency of fault-tolerant quantum error correction in light of rigorous derivations of the quantum markovian limit. *Physical Review A* **73** (2006). URL <http://dx.doi.org/10.1103/physreva.73.052311>.
 - [22] Geva, E., Kosloff, R. & Skinner, J. L. On the relaxation of a twolevel system driven by a strong electromagnetic field. *The Journal of Chemical Physics* **102**, 8541–8561 (1995). URL <http://dx.doi.org/10.1063/1.468844>.
 - [23] Esposito, M. & Gaspard, P. Emergence of diffusion in finite quantum systems. *Phys. Rev. B* **71**, 214302 (2005).
 - [24] Lewenstein, M., Mossberg, T. W. & Glauber, R. J. Dynamical suppression of spontaneous emission. *Phys. Rev. Lett.* **59**, 775–778 (1987).
 - [25] Murch, K. W. *et al.* Cavity-assisted quantum bath engineering. *Physical Review Letters* **109**, 183602+ (2012). URL <http://dx.doi.org/10.1103/physrevlett.109.183602>.
 - [26] Spohn, H. & Lebowitz, J. L. *Irreversible Thermodynamics for Quantum Systems Weakly Coupled to Thermal Reservoirs*, 109–142 (John Wiley & Sons, Inc., Hoboken, NJ, USA, 1978). URL <http://dx.doi.org/10.1002/9780470142578.ch2>.
 - [27] Alicki, R. The quantum open system as a model of the heat engine. *Journal of Physics A: Mathematical and General* **12**, L103–L107 (1979). URL <http://dx.doi.org/10.1088/0305-4470/12/5/007>.
 - [28] Spohn, H. Entropy production for quantum dynamical semigroups. *Journal of Mathematical Physics* **19**, 1227–1230 (1978). URL <http://dx.doi.org/10.1063/1.523789>.
 - [29] Esposito, M., Harbola, U. & Mukamel, S. Nonequilibrium fluctuations, fluctuation theorems, and counting statistics in quantum systems. *Rev. Mod. Phys.* **81**, 1665–1702 (2009). URL <http://dx.doi.org/10.1103/revmodphys.81.1665>.
 - [30] Esposito, M. & Parrondo, J. M. R. Stochastic thermodynamics of hidden pumps. *Physical Review E* **91** (2015). URL <http://dx.doi.org/10.1103/physreve.91.052114>.
 - [31] Raz, O., Subaşı, Y. & Jarzynski, C. Mimicking nonequilibrium steady states with time-periodic driving. *Physical Review X* **6** (2016). URL <http://dx.doi.org/10.1103/physrevx.6.021022>.
 - [32] Fogedby, H. C. & Imparato, A. A minimal model of an autonomous thermal motor. *EPL (Europhysics Letters)* **119**, 50007+ (2017). URL <http://dx.doi.org/10.1209/0295-5075/119/50007>.
 - [33] Rao, R. & Esposito, M. Detailed fluctuation theorems: A unifying perspective. *Entropy* **20**, 635+ (2018). URL <http://dx.doi.org/10.3390/e20090635>.
 - [34] Dann, R., Levy, A. & Kosloff, R. Time dependent markovian quantum master equation (2018). URL <http://arxiv.org/abs/1805.10689>. 1805.10689.